Author submitted version of article published in "Advanced Electronic Materials"
DOI: 10.100210.1002/aelm.201900205
https://doi.org/10.1002/aelm.201900205

Triboelectric-TFT flip-flop for bistable latching of dielectric elastomer actuators

*Alexis Marette, Rubaiyet Iftekharul Haque, Xiaobin Ji, Ronan Hinchet, Herbert R. Shea, Danick Briand**

Dr. A. Marette, Dr. R. I. Haque, X. Ji, Dr. R. Hinchet, Prof. H. R. Shea, Dr. D. Briand
EPFL, Rue de la Maladière, 71B, 2002-Neuchâtel, Switzerland
E-mail: danick.briand@epfl.ch
Dr. D. Briand
EPFL, Rue de la Maladière, 71B, 2002-Neuchâtel, Switzerland

Keywords: Flip-flop, triboelectric generator, high voltage thin film transistor, bistable, soft, dielectric elastomer actuator, latching

Abstract:

We report a high-voltage flip-flop combining two self-powered soft sensors with a flexible high-voltage thin film transistor (HVTFT), and use them to electrically latch dielectric elastomer actuators (DEAs) in zero and high-strain states. Two touch-actuated triboelectric generators (TENGs) are used as the gate input of a HVTFT that drives a DEA. One TENG has a positive polarity and one has a negative polarity so as to generate a voltage either higher (100 V) or lower (- 6 V) than the threshold voltage of the HVTFT. Used in a high-voltage inverter configuration, the HVTFT then controls two states for its output voltage, here 650 V (the "reset" state) and 50 V (the "set" state). When driving a DEA with actuation area strain of 19 % at 650 V, the TENG+HVTFT can latch the DEA in 2 states, at 17.5 % and 0 % strain. The 650 V output is stable, while the 50 V state drifts up to 350 V after 10 s. Due to highly non-linear strain-voltage cure of the DEA, the rise of the output voltage leads only to a 2 % increase of the DEA actuation strain in 10 s. By enabling bistable control of DEAs with TENGs, the TENG-HVTFT latch paves the ways towards automation and sensing for soft grippers and robots.

Journal article text:

The recent development of compliant grippers[1–3] and soft climbing[4] and walking robots[5,6] driven by dielectric elastomer actuators (DEAs) raise the question of how to best control those actuators. DEAs are interesting for their compliance, high-strain and fast response but generally require several kilovolts to actuate.[7,8] To enable the autonomous interaction of a DEA soft-robot with its environment, the robot requires sensors linked to high-voltage electronics. For example, a gripper requires integrated proximity sensors to detect the presence of an object in order to automatically grab it; a walking robot could integrated strain sensors in its legs for closed-loop feedback.[9]

Most stretchable sensors require analog and digital circuitry to process the signal. For example, let us consider a gripper that is intended to close when an integrated strain sensor is deformed. Mechanical contact with an object leads to the deformation of the sensor and thus to the closing of the gripper. To remain closed, the stimulus needs to be kept in memory, e.g. with a flip-flop or an electrical latch. However, the compact commercially available flip-flop gates are designed for operation below 5 V. A circuit operating at hundreds to thousands of volts to drive DEAs requires bulky power transistors. It has been shown that DEAs can be driven by flexible high voltage thin film transistors (HVTFTs)[10], so in principle a TFT-based logic gate could be developed, but the lack of complementary N and P type semiconductor technologies make the design of such a circuit complex.[11–13]

Another challenge for an autonomous soft robot is a compact flexible power supply to drive high-voltage DEAs. Soft triboelectric generators have been used to drive DEAs without high-voltage power supplies.[14,15] We will show in this communication that triboelectric generators, combined with HVTFTs, can also be used as self-powered controls to switch on and off DEAs.

The novelty of this work lies in the demonstration of a high-voltage flip-flop created by combining two self-powered triboelectric generators with a HVTFT. The triboelectric

generators, in opposite polarity configuration, can lock the HVTFT in two states, its off-state and its on-state, enabling bistable control of the high output voltage of the HVTFT. This then enables the bistable electrical latching of a 600 V DEA at 20 % area strain and at ~ 1 % area strain.

Triboelectric generators convert mechanical motion into electrical signal using contact electrification and electrostatic induction mechanism.[16] A triboelectric generator is composed of two materials having different electron/charge affinities. Initially, when contact between the functional layers occurs, charge transfer takes place from the material with lower electronegativity to the one with higher electronegativity. As a result, two layers with opposite charge are formed. Separating the layers leads to a change in voltage between the two electrodes of the triboelectric generator. A triboelectric device is a polar device, able to generate a negative and a positive voltages.[16] The generated open circuit output voltage is typically tens to hundreds of volts. As a consequence, triboelectric generators are interesting candidates for controlling the gate voltage of field effect transistors such as TFTs. Triboelectric generators integrated with TFTs form tribotronic transistors, with modulation of the output current signal by contact electrification of the gate electrode.[17,18]

The high-voltage set-reset (SR) tribotronic latch circuits and components are described in **figure 1(a)**. It consists of two triboelectric generators of opposite polarity connected in parallel to the gate electrode of a HVTFT, driving a DEA. The set triboelectric generator has smaller air gap compared to that of reset triboelectric generator. Thus, the set triboelectric generator has a higher idle capacitance than the reset triboelectric generator. Here, “set” (positive polarity) and “reset” (negative polarity) triboelectric generators refers to the triboelectric generator turning on and off the HVTFT. The HVTFT amplifies the voltage signal generated by triboelectric generators, and, in an inverter configuration, generates logic states at output. As for the equivalent flip-flop, set input, reset input, output and inverted output are called by S, R, Q and /Q, respectively.

The working principle of the Tribo-HVTFT latch is described **figure 1(b)**. When the set triboelectric generator is pressed-and-released (Stimulus on S), a positive voltage higher than the threshold voltage (V_{th}) of the transistor is generated at the gate and holds the HVTFT in on-state (Q = 1), therefore, the DEA remains in the discharged state (/Q = 0). When the reset triboelectric generator is pressed-and-released (Stimulus on R), a negative voltage lower than V_{th} is generated at the gate and holds the HVTFT in off-state (Q = 0), therefore the DEA is latched in charged state (/Q = 1).

The equivalent circuits of the tribo-HVTFT latch after triggering (pressed-and-released) of the triboelectric generators are shown in figure 2. The triboelectric generator are represented by a capacitor, C, in series with a voltage source, V_{TE}[19]. We assume that the triboelectric charge generation process was the same for both triboelectric generators, since they were fabricated at same time, using the same materials. Upon first actuation, the set triboelectric generator produced enough triboelectric charges to create a voltage higher than V_{th} across the HVTFT gate. There was no charging or transitory period necessary prior the operation of the system. The voltage generated by a triboelectric generator depends amongst other parameters on the input impedance of the circuit to which the generator is connected. Therefore, the ability of the set and the reset triboelectric generators to generate a voltage high enough to turn on and off the HVTFT gate depends on the equivalent input impedance Z of the circuit, which is the capacitance of the idle triboelectric generator in parallel with the capacitance of the HVTFT gate. The generated voltage increases with increasing resistive load but decreases with increasing capacitive load. Thus, one reaches a high voltage faster when charging a small capacitance than a large one.

In our case, for switching, one first needs the triboelectric voltage source, V_{TE}, to be higher than the threshold voltage, V_{th}, of the HVTFT. In addition, to effectively charge the HVTFT gate capacitance at a voltage higher than V_{th}, the total equivalent capacitive load Z of the circuit must be small compared to the capacitance variation of the triggered triboelectric generator. In

consequence, when the set triboelectric generator is triggered, it must match the following condition: $\Delta C_{set} = C_{set-trig} - C_{set-idle} > C_{reset-idle} + C_{HVTFT-gate}$. Where C is the capacitance and the indices $_{set, reset, trig, idle}$ refers to the set and the reset triboelectric generators in the triggered and idle state, respectively. C_{HVTFT}-gate is the HVTFT gate capacitance. The same applies when triggering the reset TENG to create a negative voltage to turn off the HVTFT. The reset TENG must follow the condition: $\Delta C_{reset} = C_{reset-trig} - C_{reset-idle} > C_{set-idle} + C_{HVTFT-gate}$. At these conditions, the voltages generated by the set and reset triboelectric generator will effectively turn on or turn off the flip-flop circuit.

The HVTFTs were designed as described in ref[10]. A cross-section of the device is provided in **figure 3(a)**. The device is built on a flexible polyimide substrate with a 10 nm thick semiconducting channel made of sol-gel zinc tin oxide (ZTO). Two electrodes made of aluminum form the source and the drain. The width of the channel between source and drain, is 5 mm, and its length is 500 µm. To minimize leakage current and to maximize the operation voltage, a gate dielectric bilayer composed of a 100 nm thick conformal Al_2O_3 layer and a 1 µm thick Parylene-C was deposited on the channel. The aluminum gate was offset from the drain by 50 µm, which enables operation at a drain voltage higher than 500 V.[10] **Figure 3(b)** shows the transfer characteristics in saturation regime at 600 V (in red) and the gate-source leakage current characteristics (in blue). The output characteristics are shown in **Figure S1**. The mobility and the on-off ratio of the HVTFT are 0.1 cm^2/Vs and 600. The threshold voltage of the transistor is of the order of 5 V.

The triboelectric generators were designed to operate in contact separation mode. A cross-section of the device is given in **figure 3(c)**. The triboelectric active layers were made of elastomers using a casting process. The PDMS layer and conductive carbon-based PDMS composite layer acted as electronegative layer. A carbon-polyurethane film was used as

electropositive layer and as second electrode. The active area of each triboelectric device is 25 cm^2. These two layers are separated by an elastomer spring to restore the air gap upon release. To experimentally fulfil the conditions on the triboelectric generator idle and triggered capacitance values expressed previously, we adjusted the spacing between the active layers of the set and reset triboelectric generator to 1 mm and 5 mm. At rest, the set triboelectric generator had a capacitance of $C_{set} = 200$ pF while the reset triboelectric generator had a capacitance of $C_{reset} = 5$ pF. When compressed, the capacitance of the set and reset triboelectric generators were 600 pF and 250 pF. The complete characteristics of the triboelectric generator output voltage and discharge time with respect to load resistance for constant mechanical force is described in **figure S2**. To measure the influence of the force and the contact time on the output voltage and the discharge time, the set triboelectric generator was placed in a mechanical push-tester with controlled force and contact time, while pressing and releasing the device. The reset triboelectric generator was connected idle in parallel. A force of 60 N was applied during 1 s. The influence of the force and the contact time on the triboelectric device output across a load are shown in **figure S3.** The voltage value increases with the contact time and the force applied to the triboelectric generator. The voltage decay time remains essentially unchanged. The signal was measured at different output loads. Under mechanical pressing, the set triboelectric generator produced negative output voltage. Then when released, a high positive voltage is generated. On the opposite, The reset TENG produced a negative voltage. The voltage then decays towards 0 V, as the charges leak through the load. **Figure 3(d)** shows the waveform of the voltage generated by a triboelectric generator with a 1 mm gap under a force of 60 N during 1 s for increasing output loads. The higher the resistive output load, the higher the peak voltage generated (55 V for 1 GΩ, 115 V for 20 GΩ). The higher the resistive output load, the longer it takes for the voltage to discharge. (2 s for 100 % discharge for 1 GΩ, around 10 s for 20 GΩ). Across a load resistance of 20 GΩ, a set output voltage of 125 V and a discharge time of 8 s was recorded.

Inversely, the reset triboelectric device generates an output voltage of – 6 V for a discharge time in the range of 10 s across a load resistance of 20 GΩ.

When actuating the triboelectric generators, the difference in the output voltages observed between the set and reset triboelectric generator was due to the difference in the input impedance of the circuit, namely the capacitive load of the idle triboelectric generator connected in parallel with the resistive load. The idle capacitance of the set triboelectric generator was 40 times higher than that of the reset triboelectric generator. In comparison to the actuation of the set triboelectric generator, the reset triboelectric generator had therefore to charge a 40 times larger capacitance load which resulted in a limited rise of its voltage in the circuit. The voltage output was in all cases sufficient to switch the HVTFT on and off.

To demonstrate that the tribo-HVTFT flip-flop can electrically latch DEAs, we designed as a general demonstrator a circular expanding in-plane DEA under equibiaxial pre-stretch. The DEAs were designed to reach their maximum actuation strain at 700 V, corresponding to an electric field of 120 V/μm. Reduction of the DEA operation voltage could be obtain by decreasing the dielectric thickness[20,21] or by increasing the dielectric constant of the dielectric.[22] Our approach can be generalized to a DEAs with a higher operation voltage if the HVTFT is made also to withstand higher drain-source voltage.[10] A cross-section of the device is shown in **figure 3(e)**. It is composed of a PDMS layer with a thickness of 6 μm sandwiched between two carbon-black composite electrodes of 2 μm thickness[21]. The area strain – voltage characteristics is plotted in **figure 3(f)**. Under the application of 650 V, the device achieves 19 % area strain.

We connected the components together as shown in **figure 4(a)**. Before starting the measurement, the triboelectric generator flip-flop output was connected to the ground to discharge the HVTFT gate capacitor, so that the initial gate voltage was 0 V. To measure the open-circuit output voltage of the triboelectric generator flip-flop, we connected its output to a high input impedance voltage amplifier (20 GΩ). The output chronogram is shown in **figure**

4(b). Triggering the set triboelectric generator latches the output voltage between 50 and 100 V and triggering the reset triboelectric generator latches the output voltage between 0 and 5 V. The triboelectric generators were manually pressed without control over the force, which explains the variability in output voltage. The drop of voltage observed in the high-voltage region can be attributed to charge leakage through the load resistance.

By connecting a pull-up 1 GΩ bias resistor to the HVTFT we obtain the inverter output characteristics shown in **figure 4(c)**. The gate voltage of the HVTFT has to be less than 10 V for it to remain off, and above 50 V to remain on, which corresponds to the TENG flip-flop output described above. **Figure 4(d)** shows the output response of the DEA under set and reset latching over several cycles, demonstrating the stability of the latching effect over several cycles. The chronogram is described in detail in **figure 4(e)**. When the reset-triboelectric is pressed and released, the output voltage of the HVTFT is latched at 650 V resulting to a 17.5 % area strain on the DEA. This value remained stable for several minutes. When the set-triboelectric is pressed and released the initial value of the output voltage sets at 50 V and the DEA area strain drops to 0 %. Then it increases to 350 V after 10 s leading to a slight increase of the DEA area strain to 2 %. This may be due to charge leakage through the gate dielectric of the HVTFT and the triboelectric device. This leads to the gradual drop of the gate voltage of the HVTFT.

In summary, we have demonstrated the first electromechanical high voltage flip-flop made of a pair of triboelectric generators and a HVTFT. This electrical latch amplifies the triboelectric stimuli to hold an external DEA in two stable states, actuated and not actuated. We demonstrated our approach using a DEA working at 650 V, showing 17.5 % area strain latching after having pressed and released the reset triboelectric device and 2 % area strain latching after having pressed and released the set triboelectric device. This approach could be extrapolated to kV DEAs, if the breakdown voltage of the HVTFT was increased towards this voltage by gate shifting or dielectric layer optimization. Future improvements would consist

in optimizing the HVTFT to avoid gate-source current leakage and in using YZTO HVTFTs[23], to increase the HVTFT channel current, while keeping a high on-off ratio at high-voltage. Additionally, miniaturization of the triboelectric generator will be necessary for future integration in complex soft robots. In order to generate a high control voltage with stretchable triboelectric generators, high dielectric constant with high electron affinity materials serving as triboelectric layers such as the ones described in Yu et al. could be implemented.[24] By integrating this tribo-HVTFT flip-flop in soft grippers and mobile robots driven by DEAs, this work paves a way towards sensing logic for soft robots based on DEAs and other high-voltage devices such as electrostatic actuators[25] and electro-adhesion devices.[26]

Experimental section

The fabrication and the dimension of the active layers of the triboelectric devices are described in **Figure S4** and are based on.[27] Soft dielectric elastomers, polydimethylsiloxane (PDMS) (Sylgard 186, DowCorning) and electrically conductive carbon-polyurethane (CPU), having opposite charge affinities were used as triboelectric layer. Electrically conductive carbon-PDMS (CPDMS) was used as electrode for PDMS layer. Both CPDMS and CPU were prepared by dispersing 10 wt.% of carbon-black particles (Ketjenblack EC600JD) into PDMS and polyurethane (MM4520, SMP Technology Inc.) elastomers. The different functional layers were deposited by blade-casting. A sacrificial layer made of PAA (Sigma-Aldrich, 5% diluted in isopropanol) is deposited on a PET substrate. On top of this layer a PDMS layer is deposited to act as a protective layer. Thereafter, a CPDMS layer and another PDMS layer were deposited, forming the electronegative triboelectric-electrode layer. For the electropositive triboelectric structure, a multilayer PU-CPU functional structure is formulated, where the initial PU layer acts as protective layer and CPU layer acts both as the triboelectric layer and electrode. Curing was performed at 80 °C for 2 hours. Thereafter, the functional

layers were assembled facing each other utilizing SILRES PSA 45559 VP silicone pressure-sensitive adhesive (Wacker), and a thick layer of PDMS (Sylgard 186 silicone elastomer, DowCorning) folded in arc shape. The arc form enabled an air spacer by maintaining the separation between the electropositive and electronegative layer. The gap was 1 mm for the set triboelectric generator, 5 mm for the reset triboelectric generator.

The HVTFT was fabricated as described in ref[10,23]. The DEAs were fabricated using a similar fabrication process as in ref[28]. The DEA consisted of a 6.5 µm thick PDMS (Sylgard 186, DowCorning) membrane sandwiched between two layers of 2 µm thick pad-printed carbon-PDMS electrodes. The active area was 4 mm diameter and the membrane prestretch was 1.3. As reported by Saint-Aubin et al., DEAs made with similar materials are robust and show less than 1 % change in generated strain after more than 5 million of actuation cycles.[29]

Supporting Information

Supporting Information is available from the Wiley Online Library or from the author.

Acknowledgements

This work was supported by the Swiss National Science Foundation (Grant No. 200020-165993) and by the European Union's Horizon 2020 research and innovation program under the Marie Skłodowska-Curie grant agreement No 641822—MICACT via the Swiss State Secretariat for Education, Research, and Innovation. The authors thank the EPFL-CMi staff for the TFT microfabrication and the EPFL-LMTS team for helpful comments and discussion.

Received: ((will be filled in by the editorial staff))
Revised: ((will be filled in by the editorial staff))
Published online: ((will be filled in by the editorial staff))

References

[1] S. Shian, K. Bertoldi, D. R. Clarke, *Adv. Mater.* **2015**, *27*, 6814.
[2] J. Shintake, S. Rosset, B. Schubert, D. Floreano, H. Shea, *Adv. Mater.* **2016**, *28*, 231.
[3] J. Shintake, V. Cacucciolo, D. Floreano, H. Shea, *Advanced Materials* **2018**, *30*, 1707035.
[4] J. Cao, L. Qin, J. Liu, Q. Ren, C. C. Foo, H. Wang, H. P. Lee, J. Zhu, *Extreme Mechanics Letters* **2018**, *21*, 9.
[5] M. Duduta, D. R. Clarke, R. J. Wood, in *2017 IEEE International Conference on Robotics and Automation (ICRA)*, **2017**, pp. 4346–4351.

[6] C. T. Nguyen, H. Phung, T. D. Nguyen, C. Lee, U. Kim, D. Lee, Hyungpil Moon, J. Koo, J. Nam, H. R. Choi, *Smart Mater. Struct.* **2014**, *23*, 065005.
[7] R. Pelrine, R. Kornbluh, Q. Pei, J. Joseph, *Science* **2000**, *287*, 836.
[8] S. Rosset, H. R. Shea, *Applied Physics Reviews* **2016**, *3*, 031105.
[9] M. Amjadi, K.-U. Kyung, I. Park, M. Sitti, *Advanced Functional Materials* **2016**, *26*, 1678.
[10] A. Marette, A. Poulin, N. Besse, S. Rosset, D. Briand, H. Shea, *Adv. Mater.* **2017**, *29*, 1700880.
[11] J. Noh, M. Jung, K. Jung, G. Lee, J. Kim, S. Lim, D. Kim, Y. Choi, Y. Kim, V. Subramanian, G. Cho, *IEEE Electron Device Letters* **2011**, *32*, 638.
[12] E. Fortunato, P. Barquinha, R. Martins, *Advanced Materials* **2012**, *24*, 2945.
[13] Y. Takeda, K. Hayasaka, R. Shiwaku, K. Yokosawa, T. Shiba, M. Mamada, D. Kumaki, K. Fukuda, S. Tokito, *Scientific Reports* **2016**, *6*, 25714.
[14] X. Chen, T. Jiang, Y. Yao, L. Xu, Z. Zhao, Z. L. Wang, *Adv. Funct. Mater.* **2016**, *26*, 4906.
[15] X. Chen, Y. Wu, A. Yu, L. Xu, L. Zheng, Y. Liu, H. Li, Z. Lin Wang, *Nano Energy* **2017**, *38*, 91.
[16] F.-R. Fan, Z.-Q. Tian, Z. Lin Wang, *Nano Energy* **2012**, *1*, 328.
[17] C. Zhang, J. Li, C. B. Han, L. M. Zhang, X. Y. Chen, L. D. Wang, G. F. Dong, Z. L. Wang, *Advanced Functional Materials* **2015**, *25*, 5625.
[18] C. Zhang, Z. L. Wang, *Nano Today* **2016**, *11*, 521.
[19] R. Hinchet, A. Ghaffarinejad, Y. Lu, J. Y. Hasani, S.-W. Kim, P. Basset, *Nano Energy* **2018**, *47*, 401.
[20] A. Poulin, S. Rosset, H. R. Shea, *Applied Physics Letters* **2015**, *107*, 244104.
[21] X. Ji, A. El Haitami, F. Sorba, S. Rosset, G. T. M. Nguyen, C. Plesse, F. Vidal, H. R. Shea, S. Cantin, *Sensors and Actuators B: Chemical* **2018**, *261*, 135.
[22] D. M. Opris, *Advanced Materials* **2018**, *30*, 1703678.
[23] A. Marette, H. R. Shea, D. Briand, *Appl. Phys. Lett.* **2018**, *113*, 132101.
[24] A. Yu, Y. Zhu, W. Wang, J. Zhai, *Advanced Functional Materials* **n.d.**, *0*, 1900098.
[25] E. M. Chow, J. P. Lu, J. Ho, C. Shih, D. De Bruyker, M. Rosa, E. Peeters, *Sensors and Actuators A: Physical* **2006**, *130–131*, 297.
[26] L. Xu, H. Wu, G. Yao, L. Chen, X. Yang, B. Chen, X. Huang, W. Zhong, X. Chen, Z. Yin, Z. L. Wang, *ACS Nano* **2018**, DOI 10.1021/acsnano.8b05359.
[27] R. I. Haque, P.-A. Farine, D. Briand, *Sensors and Actuators A: Physical* **2018**, *271*, 88.
[28] S. Rosset, O. A. Araromi, S. Schlatter, H. R. Shea, *JoVE (Journal of Visualized Experiments)* **2016**, e53423.
[29] C. A. de Saint-Aubin, S. Rosset, S. Schlatter, H. Shea, *Smart Mater. Struct.* **2018**, *27*, 074002.

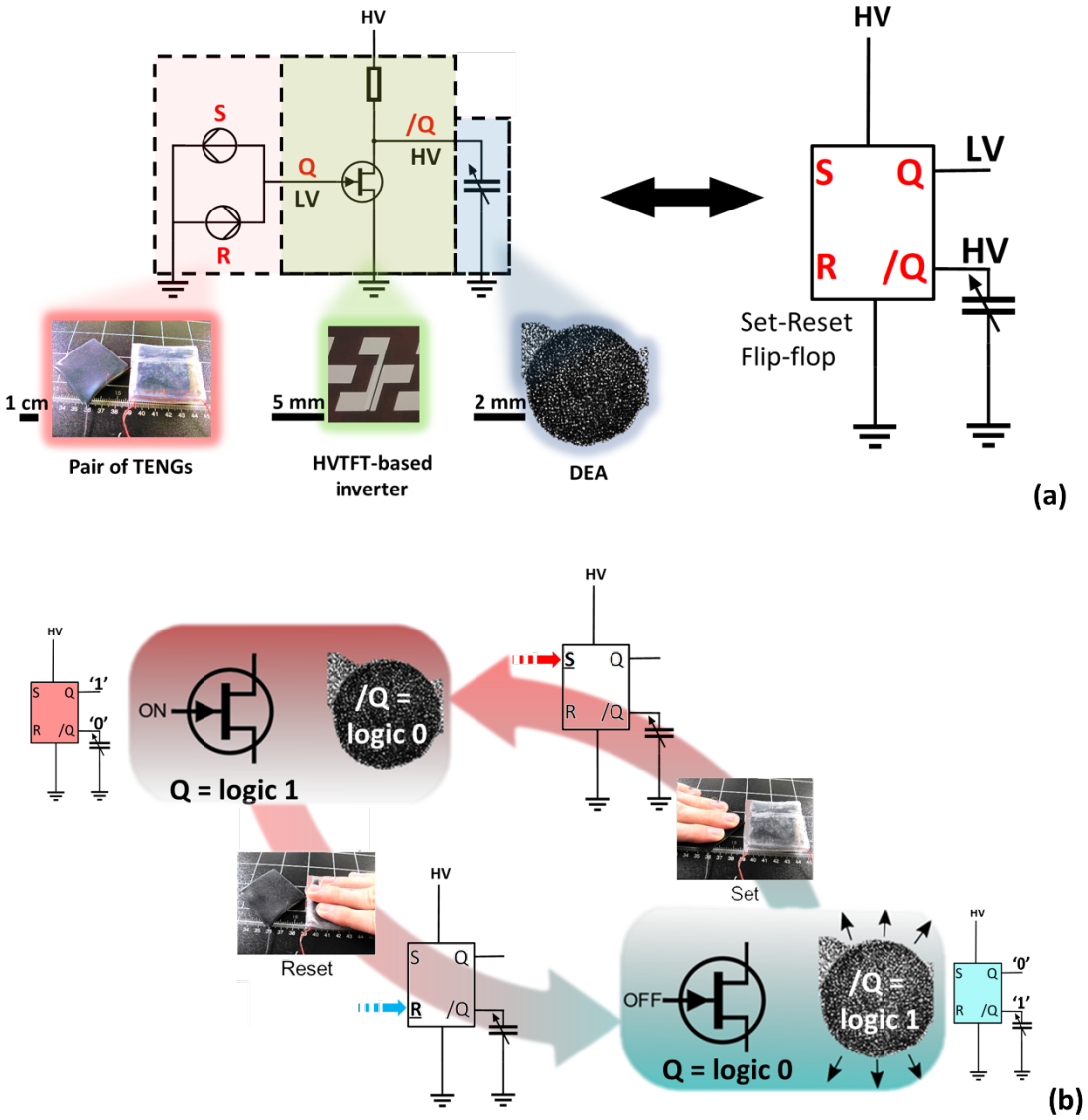

Figure 1. (a) Electrical schematic and equivalent circuit of the tribo-HVTFT flip-flop driving a DEA. A pair of triboelectric generators of opposite polarity controls the HVTFT gate voltage. The HVTFT, in inverter configuration, controls the state of the DEA and provides an inverted high voltage output to the triboelectric stimuli. This entire configuration is equivalent to a high-voltage flip-flop. (b) Working principle of the tribo-HVTFT flip-flop driving a DEA. When we press on the set triboelectric device, the DEA is electrically latched in a discharged state. When we press on the reset triboelectric, the DEA is latched in a charged state.

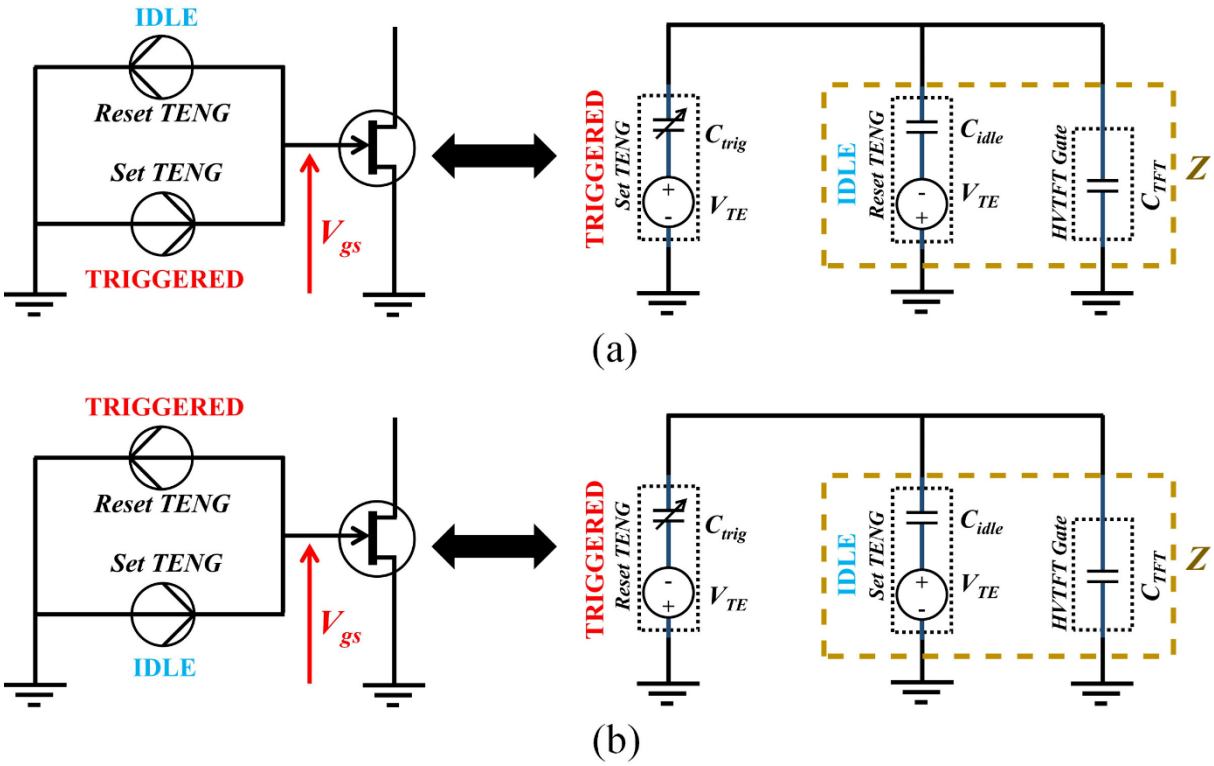

Figure 2. Equivalent circuit of the tribo-HVTFT latch, while: **(a)** the set triboelectric generator is triggered, and **(b)** the reset triboelectric generator is triggered.

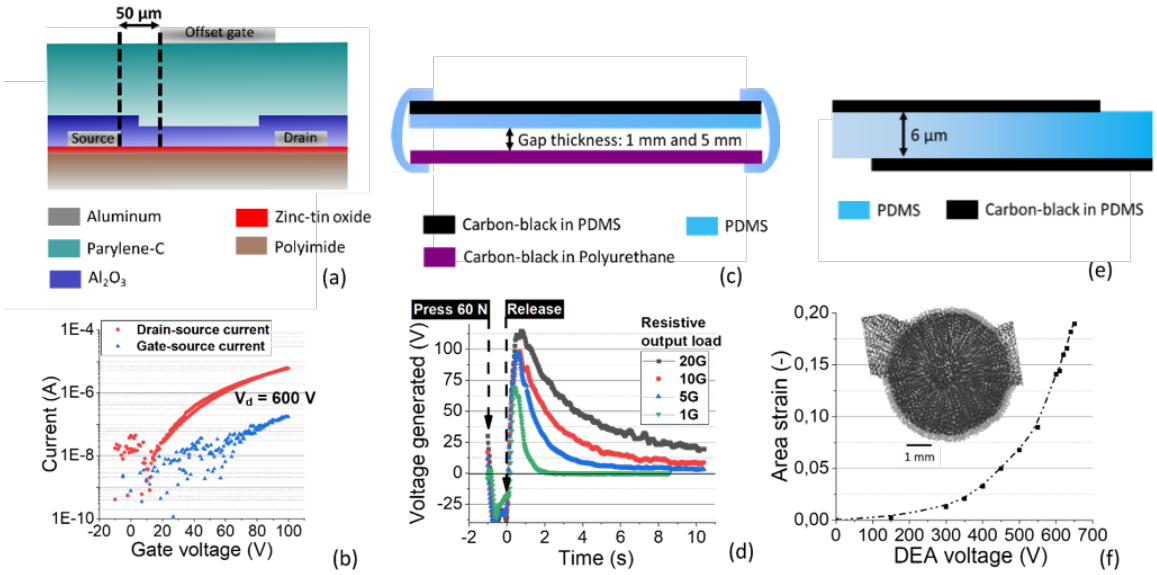

Figure 3. (a) Cross-section of the HVTFT. (b) Transfer characteristics of the HVTFT. (c) Cross-section of a triboelectric generator. The set triboelectric generator has a 1 mm gap and the reset triboelectric generator has a 5 mm gap. (d) Characteristics of the set triboelectric generator as a function of its output load. (e) Cross-section of the DEA. (f) Area strain vs voltage applied across the DEA.

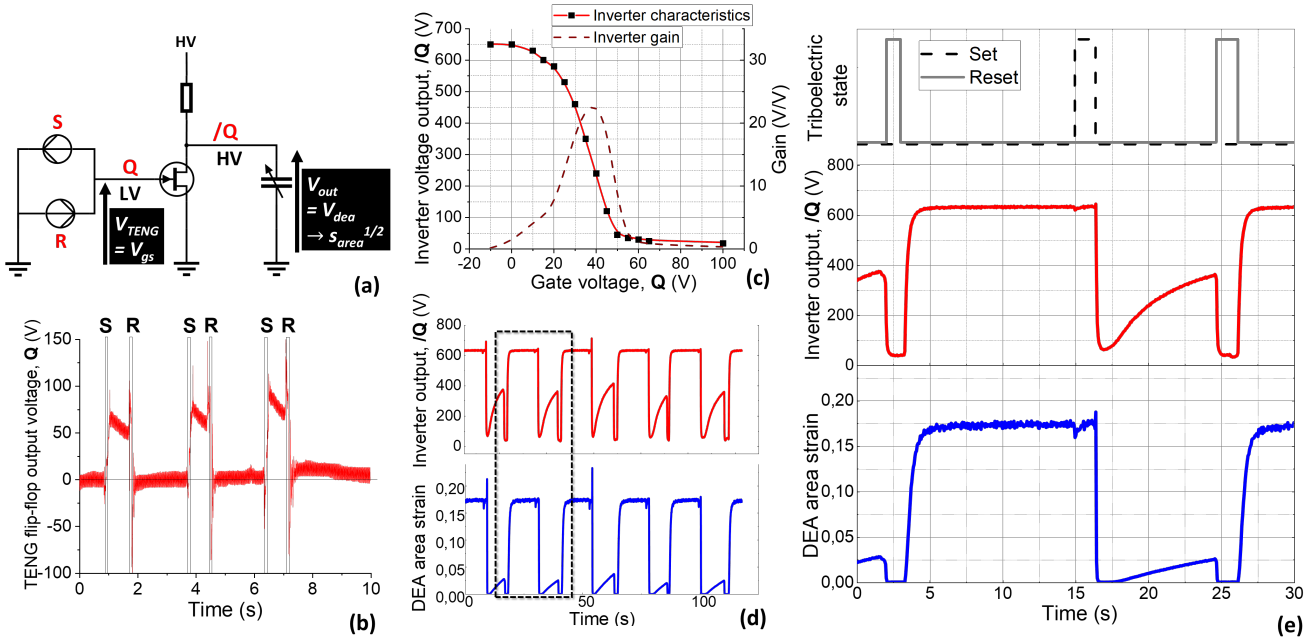

Figure 4. (a) Circuit of the tribo-HVTFT latch driving the DEA. (b) Output voltage of the high voltage flip-flop connected to a 20 GΩ load. (c) Amplification characteristics of the HVTFT to drive the DEA. (d) Chronogram of 5 latching cycles of the complementary tribo-HVTFT latch on the DEA. (e) Chronogram of the DEA output voltage and area strain vs the triboelectric stimuli.

The table of contents entry should be 50−60 words long, and the first phrase should be bold.

We report a high-voltage flip-flop combining two self-powered soft sensors with a flexible high-voltage thin film transistor (HVTFT). They are used to electrically latch dielectric elastomer actuators (DEAs) in zero and high-strain states. By enabling bistable control of DEAs with triboelectric generators, the tribo-HVTFT latch paves the ways towards automation and sensing for soft grippers and robots.

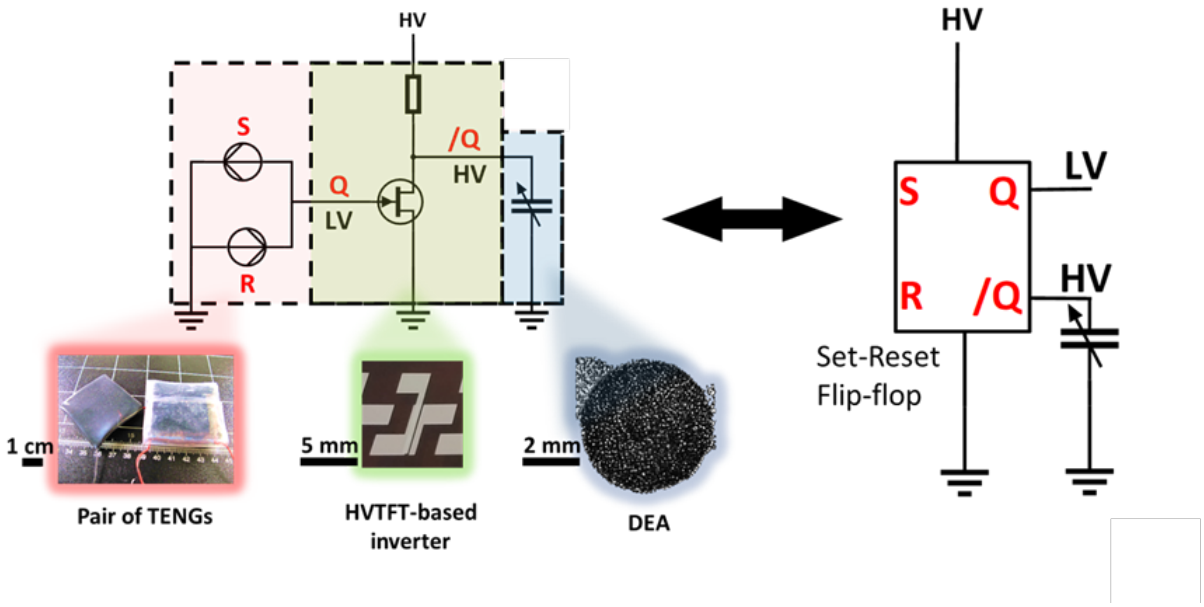

Flip-flop, triboelectric generator, high voltage thin film transistor, soft, dielectric elastomer actuator.
A. Marette, R.I. Haque, X. Ji, D. Briand, H. R. Shea*

Triboelectric-TFT flip-flop for bistable latching of dielectric elastomer actuators

((Supporting Information can be included here using this template))

Supporting Information

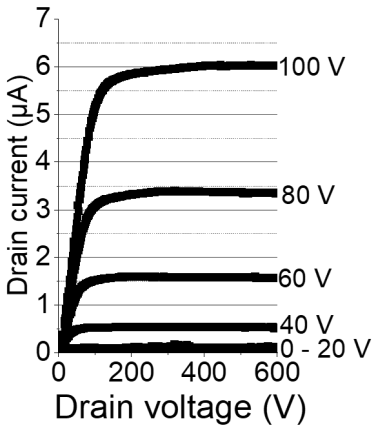

Figure S1. Output characteristics of the HVTFT.

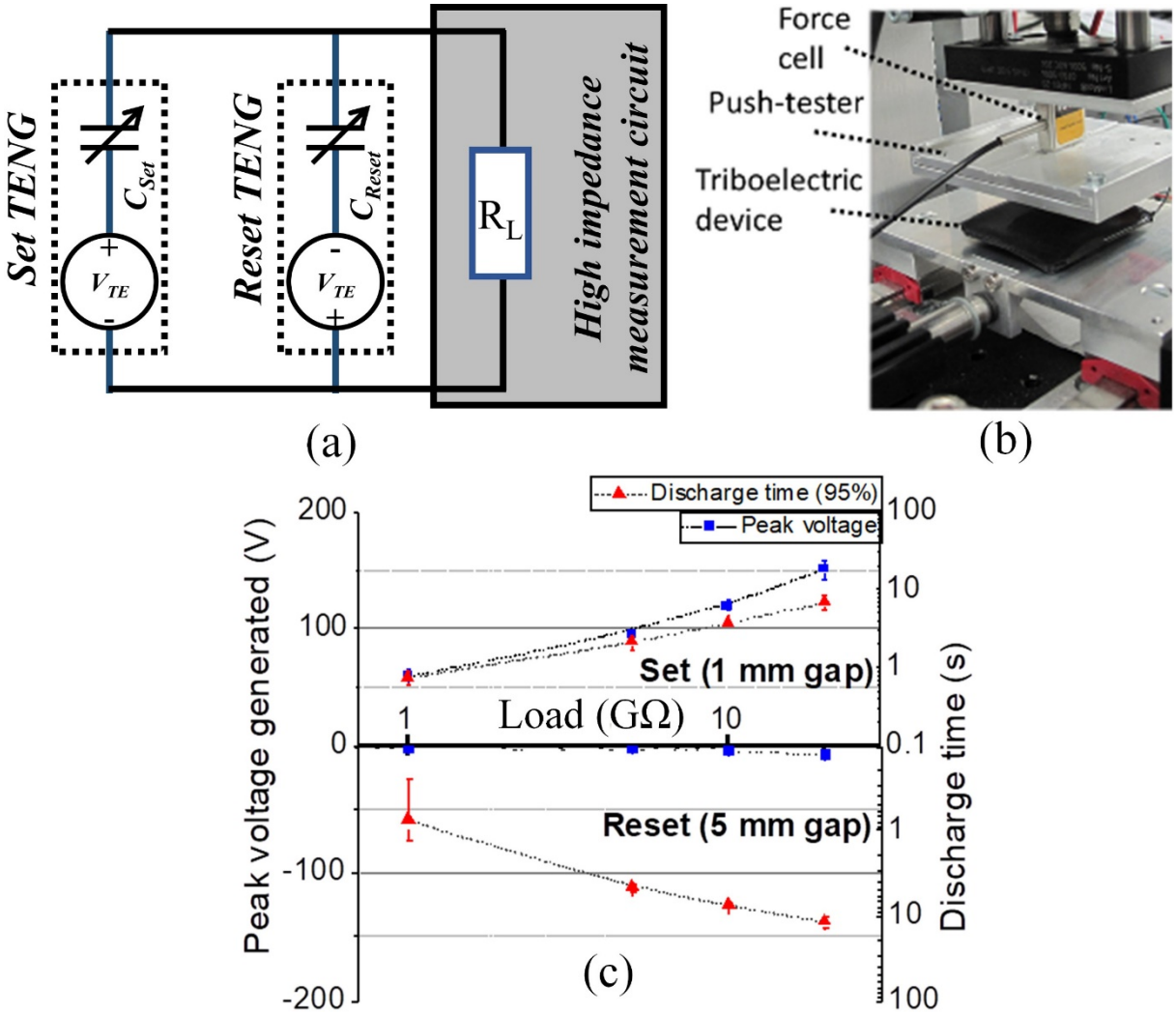

Figure S2. (a) Schematic of the electrical setup to characterize the individual triboelectric generators when connected in flip-flop configuration and **(b)** photograph of the experimental setup. The characterization of the triboelectric generator was performed using a linear motor based mechanical setup. The piston was used to create vertical stimuli on the triboelectric generators. The load resistance (R_L) was changed manually, and the output voltage and discharge time were recorded using an oscilloscope. When the set triboelectric generator was excited by mechanical stimuli, the reset triboelectric generator remain idle, and vice versa. **(c)** Triboelectric output voltage with respect to load, under latching of the set and reset triboelectric generators, for the constant force of 60 N, connecting in flip-flop configuration.

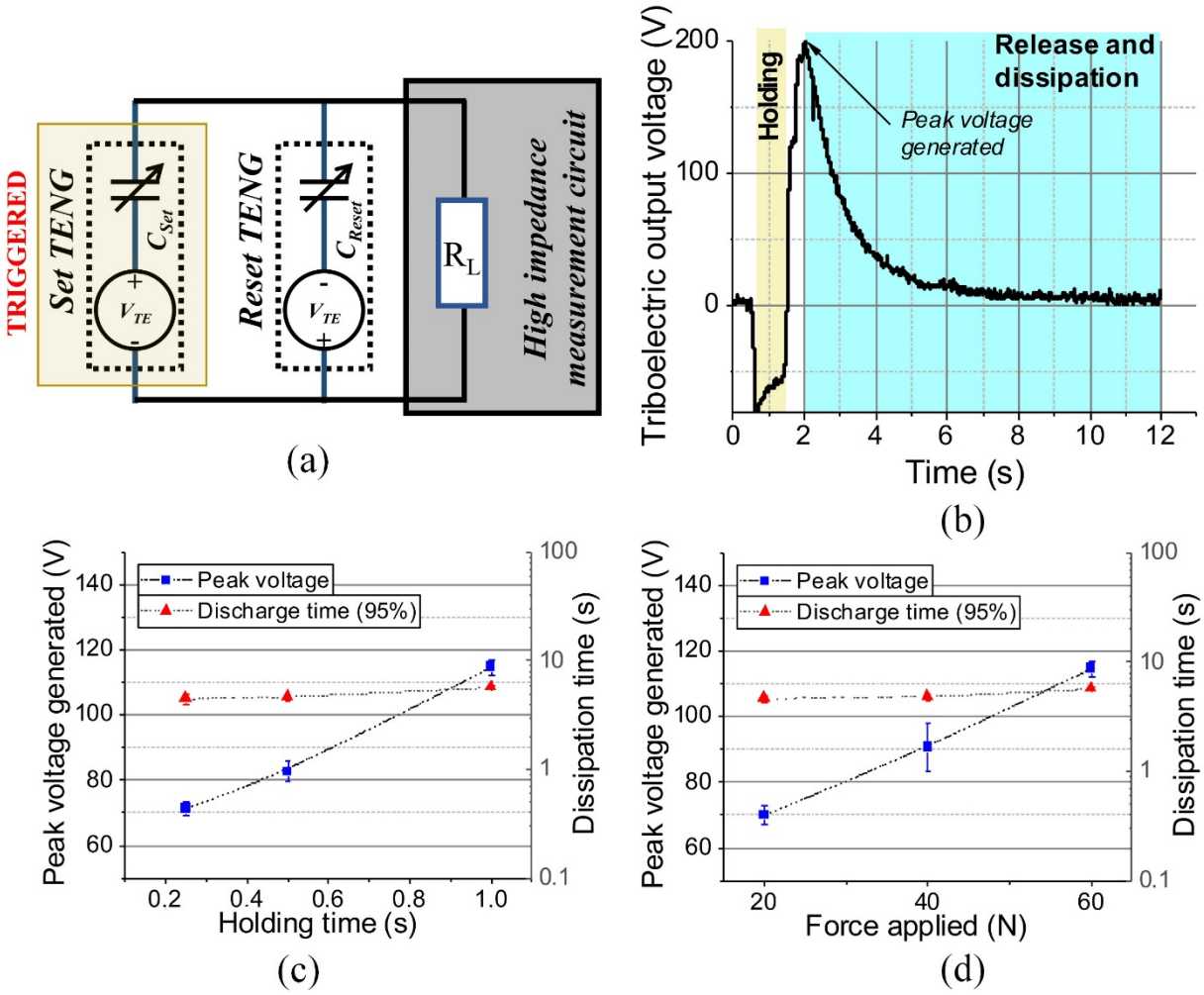

Figure S3. (a) Schematics of the setup used to characterize the triboelectric generator based latching. **(b)** Set triboelectric output voltage with respect to time describing a pressing cycle for a load of 20 GΩ. The yellow region corresponds to the voltage generated by the triboelectric device when it is pressed. The blue region corresponds to the voltage generated after release (the latching state). **(c)** Plot of the set voltage generated when released and the time taken to go back to 5% of the maximum voltage vs. the contact time in pressed mode across a constant load of 20 GΩ. **(d)** Plot of the set voltage generated across a constant load of 20 GΩ when released and the time taken to go back to 5% of the maximum voltage with respect to the force applied in pressed mode.

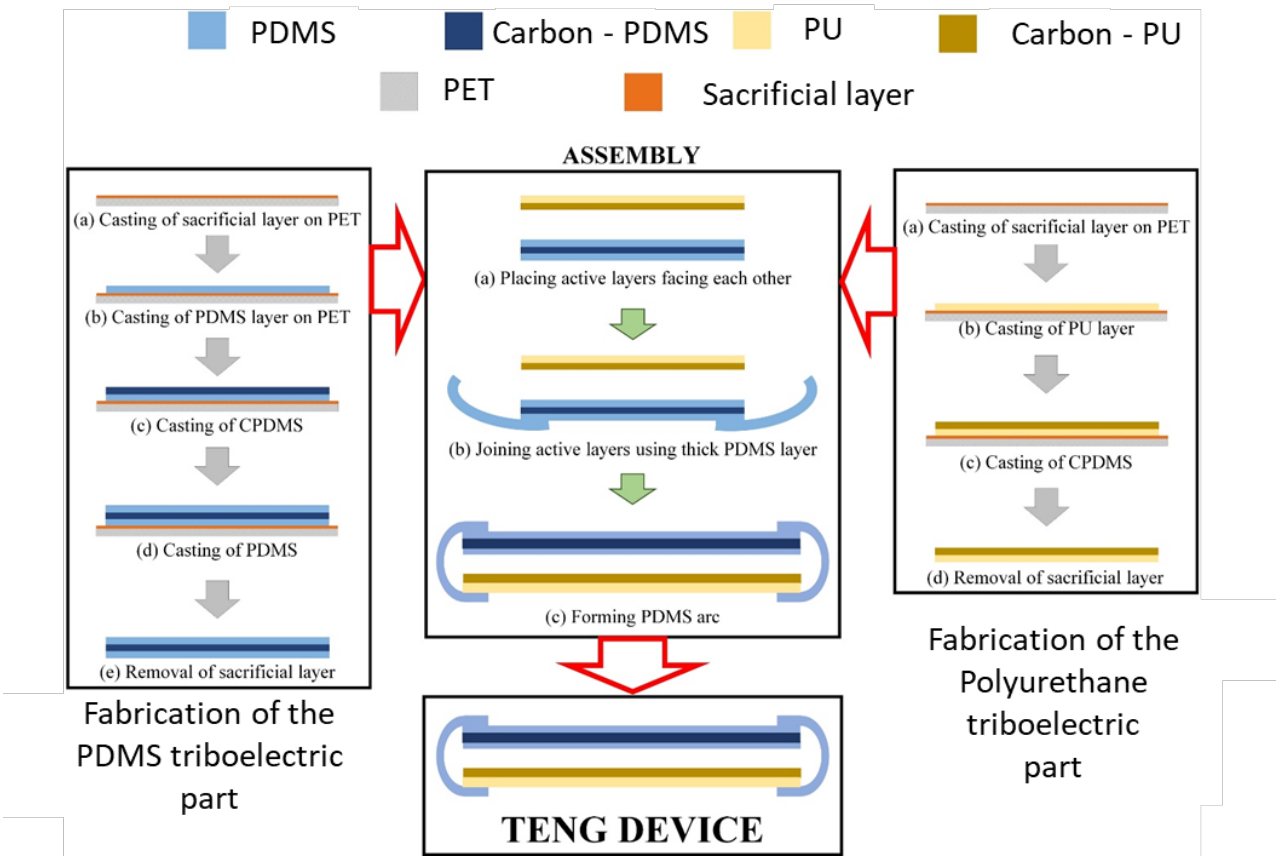

Physical parameters	TENG-A	TENG-B
Area [cm^2]	25	25
Spacer height [mm]	1	8
Thickness of PDMS [μm]	62.0±2.4	62.0±2.4
Thickness of CPDMS [μm]	30.6±2.3	30.6±2.3
Thickness of PU [μm]	31.0±2.0	31.0±2.0
Thickness of CPU [μm]	11.0±2.0	11.0±2.0

Figure S4. Fabrication process of a triboelectric device and table of the dimensions of the functional layers.